Energy Proceedings
Vol 50, 2025
ISSN 2004-2965

A comprehensive 3-D proton exchange membrane water electrolysis cell model: An optimization perspective[#]

Liulin Que[1,2], Yanyan Huang[1,2], Liang Zhang [1,2*], Jun Li[1,2], Dingding Ye[1,2], Jian Huang[1,2], Xun Zhu[1,2], Qiang Liao[1,2]

1 Key Laboratory of Low-grade Energy Utilization Technologies and Systems, Chongqing University, Ministry of Education, Chongqing 400030, China

2 Institute of Engineering Thermophysics, School of Energy and Power Engineering, Chongqing University, Chongqing 400030, China

(Corresponding Author: liangzhang@cqu.edu.cn)

ABSTRACT

Proton exchange membrane water electrolysis (PEMWE) have received great attention for renewable hydrogen production. In present work, a 3D multi-phase, non-isothermal cell-level model that consider all the physical characteristics in water electrolysis, such as liquid water transport, proton transport in membrane electrode assembly (MEA), electron transport in solid electrode, gas diffusion in porous electrodes, water evaporation, dissolved water transport in MEA and hydrogen permeation from cathode to anode. The numerical results show good agreement with experimental data. The validated model is used to analyze the effect of key operating conditions on the voltage losses and efficiency. T_0 = 80 °C is optimal for the full range of operating current densities. However, as current density increases, lower temperatures become more beneficial for performance. Performance can be improved through the development of CLs with good activity, especially on the anode side. The above findings provide the characteristics of gas distribution and the influencing mechanisms of key parameters within the cell, providing a theoretical foundation for optimal design of PEMWE.

Keywords: PEM water electrolysis, modeling, efficiency, temperature, optimization

NONMENCLATURE

Abbreviations	
PEM	Proton exchange membrane
MEA	Membrane electrode assembly
CFD	Computational fluid dynamics
Symbols	
T_0	Inlet water temperature
i_0	Exchange current density

1. INTRODUCTION

Water electrolysis is a promising technology for the green hydrogen production, providing a low-carbon emission solution despite being approximately twice as expensive as industrial hydrogen production from natural gas [1]. Water electrolysis technologies are generally classified into three types: proton exchange membrane (PEM) water electrolysis, alkaline water electrolysis, and solid oxide electrolysis. Proton exchange membrane water electrolysis (PEMWE) technology offers significant advantages, including high current density, high energy conversion efficiency, and strong compatibility with renewable energy sources, making it a leading area of research in large-scale energy storage [2,3]. However, the implementation of PEMWE presents several challenges. It necessitates the use of costly noble metal catalysts and operates under stringent conditions characterized by high current densities, strong acidity, and complex gas-thermal-electric multicomponent interactions [4,5].

Advancing the performance and reducing the cost of PEM water electrolysis technology can enable its widespread industrial application for energy conversion and storage. Computational fluid dynamics (CFD) simulation plays a crucial role in this process by offering valuable insights into design modifications and optimizing operational parameters [6]. Toghyani et al. [7] (2018) conducted a study on the performance of PEMWE, comparing five different channel patterns. Olesen et al. [8] (2019) developed a comprehensive 3D macroscopic model including detailed geometry of the flow field. They concluded that cell performance is largely influenced by anode dynamics, film thickness and electrical contact resistance. Chen et al. [9] (2020) developed a multi-physics CFD model to analyze the

This is a paper for the 16th International Conference on Applied Energy (ICAE2024), Sep. 1-5, 2024, Niigata, Japan.

two-phase flow and electrochemical interactions in the anode PTL of a PEMWE, revealing liquid water distribution, local current density, and performance variations with different PTL thicknesses. Lin and Zausch [10] (2022) developed a 1D model to analyze two-phase flow, electrochemical processes, and material property impacts on electrochemical performance, hydraulic behavior, and water management in anode components. Pablo A. [11] (2023) utilized a comprehensive 1D two-phase, non-isothermal model to analyze critical aspects of PEMWE technology, validate it against experimental data, and conduct a parametric analysis to identify essential design parameters for enhanced performance. Current modeling deficiencies are primarily reflected in three areas. Firstly, only the generation and diffusion of single gases at the anode and cathode are considered, whereas water evaporation and gas permeation also impact electrolysis performance. Second, many studies assume the membrane is fully hydrated, but in practice, its water content varies, especially under high current density, leading to membrane drying. Most models are based on 1D and 2D calculations, which fail to capture the in-plane distribution of substances.

In this study, we propose a comprehensive 3-D two-phase, non-isothermal macroscopic model. The model rigorously analyzes the transport phenomena of three distinct phases of water, including liquid water, vapor, and dissolved phases, and their intricate interconversion processes. Furthermore, it delves into the infiltration of hydrogen gas at the cathode, thereby enriching our comprehension of the intricate transport dynamics within the PEMWE system. This model is formulated and compared with experimental data, and then a parametric analysis is carried out in terms of operating conditions and electrochemical parameters. Overall, the work provides mechanism analysis and a perspective of key design parameters for improving PEMWE performance.

2. MATHEMATICAL MODELING DESCRIPTION

2.1 Physical model

As depicted in Fig. 1, the schematic illustrates a classical single-flux 3D PEMWE with parallel channels on both the anode and cathode sides. The model comprises an anode bipolar plate (ABP), a cathode bipolar plate (CBP), an anode flow channel (ACH), a cathode flow channel (CCH), liquid/gas porous transport layers at the anode and cathode (APL and CPL), catalyst layers at the anode and cathode (ACL and CCL), and a proton exchange membrane (PEM). The origin of the x/y/z axis is positioned at the outermost inlet of the CBP, increasing along the width direction, the flow direction, and the thickness direction, respectively.

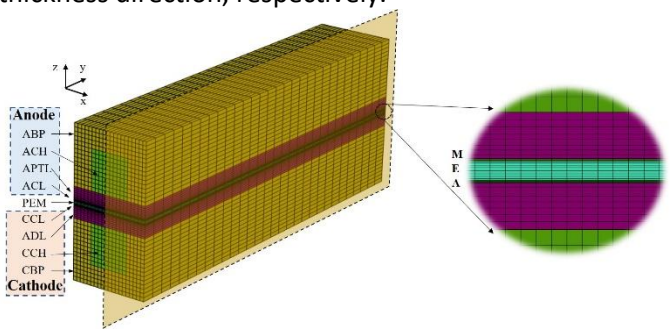

Fig. 1 Schematic representation of the 3-D model

During the operation of the cell, liquid water flows through the ACH and diffuses through the APL to the ACL. Water molecule is then generated into protons, electrons and oxygen as shown in equation (1). The produced protons enter the CCL through the PEM under the electric field force and react with electrons from the external circuit as shown in equation (2). On the cathode side, liquid water is introduced into the CCH because it enhances hydrogen evacuation and prevents membrane drying, especially at high current densities.

$$H_2O \rightarrow 2H^+ + \frac{1}{2}O_2 + 2e^- \quad (1)$$

$$2H^+ + 2e^- \rightarrow H^2 \quad (2)$$

2.2 Conservation equations and transport properties

The model is composed of eleven conservation equations: (i–ii) mass and (iii–iv) momentum of liquid and gas phases, (v) species transfer of gas, (vi) electronic charge, (vii) protonic charge, (viii) liquid water saturation conservation, (ix) dissolved water in electrolyte, (x) hydrogen cross-over and (xi) energy. All the equations used in the model are from literatures [1,2,4,9].

3. MODEL VALIDATION AND NUMERICAL IMPLEMENTATION

To validate the numerical model, it was first utilized to calculate the polarization performance of PEMWE based on experimental conditions tested in reference [12] and our experimental data. The polarization curves of the cell at different temperatures (25, 45 and 80 °C) from simulation and experimental data are compared in Fig. 2(a). The model was validated simultaneously with experimental data with inlet water temperature of T_0 = 80 °C (yellow line with cyan dot). Different voltage losses have been calculated and compared with experimental values and are within reasonable limits., as shown in Fig. 2(b). The computed results demonstrate good agreement with the experimental data.

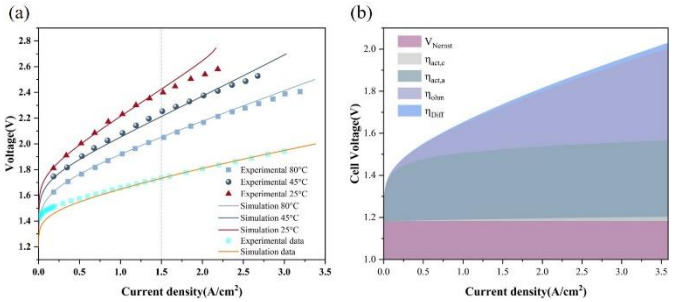

Fig. 2 (a) Predicted polarization curves compared to the experimental data at different temperatures (25, 45 and 80 °C) and experimental data at 80 °C (cyan dot); (b) Breakdown of volage loss at 80 °C, ΔV

4. RESULTS AND DISCUSSION

4.1 Basic gas distribution characteristic

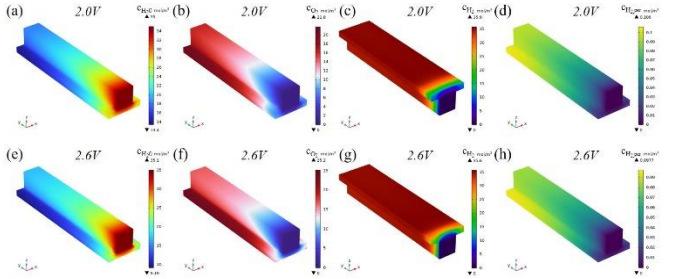

Fig. 3. Variations of distributions of vapor, oxygen, hydrogen, permeation hydrogen under different voltage condition (a-d) V_0 *= 2.0 V, (e-h)* V_0 *= 2.6 V*

Oxygen and hydrogen are primarily generated during the operation of the electrolysis tank, while vapor results from the evaporation of liquid water due to increased temperature and decreased saturation pressure. Additionally, hydrogen generated at the cathode penetrates to the anode. Monitoring the distribution of different gas components throughout the experimental process is challenging due to their mutual interactions. Thus, it is essential to clarify the distribution patterns and the percentage of each component.

Fig. 3 show the distributions of the concentrations of vapor, oxygen, and hydrogen in the cathode, as well as hydrogen in the anode. As shown in Fig. 3(a) and (e), water evaporation occurs throughout the anode (the cathode not shown). The water supplied to the anode leads to the evaporation of liquid water, followed by the immediate sorption of liquid water and vapor into the ionomer. High vapor concentration areas are mainly found at the flow inlet, with relatively high concentrations throughout the ACH due to the low saturation vapor pressure of the water at the inlet. Meanwhile, the vapor concentration decreases along the flow direction due to changes in the partial pressure of vapor and saturation pressure, resulting in condensation. From Fig. 3(b) and (f), the tendencies of oxygen molar concentration in the anode are opposite to those of vapor and liquid water saturation. These distributions are mainly caused by the chemical reactions occurring in the ACL. Oxygen diffuses into the ACH through the APL and is swept away by the water flow. Consequently, oxygen gradually accumulates along the ACH, leading to a decrease in liquid water saturation and vapor percentage. The tendencies of hydrogen molar concentration are similar to oxygen, but with a smaller gradient and higher concentration in the cathode due to faster hydrogen diffusion and higher production rate, as shown in Fig. 3(c) and (g). From Fig. 3(d) and (h), the hydrogen concentration distribution in the anode is consistent with that in the cathode, though the latter is much more concentrated. While most of the hydrogen produced at the cathode is eventually transported in gaseous form, some penetrates the membrane to reach the anode. The higher hydrogen concentration at the anode along the flow direction is due to the higher hydrogen concentration on the symmetrical side of the cathode.

4.2 Parametric analysis

The results of the parametric analysis of the operation and electrochemical parameters are presented separately in the next section. In all cases, it is shown the effect on polarization curve and PEMWE efficiency.

4.2.1 *Operation conditions*

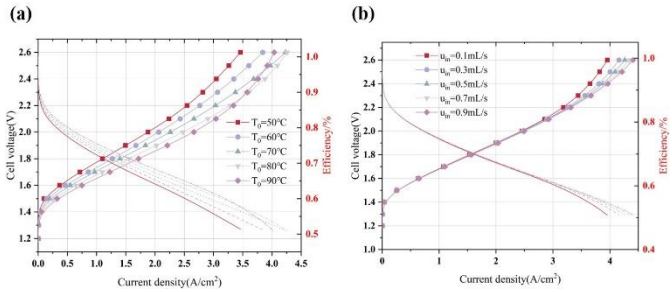

Fig. 4. Effect of operating temperature on polarization curve and efficiency, (a) T_0 *= 50, 60,70, 80, 90* °C*, (b) water inlet rate* Q_{in} *= 0.1-0.9 mL/s.*

Fig. 4 shows the results of the analysis of operating temperature, T_0, and inlet flow, Q_{in}. For temperatures varying between 50 and 70 °C, Fig. 4(a) shows that the PEMWE performance improved significantly as the inlet water became warmer, it is due to the temperature minimized the activation and Ohmic losses to offset the mass transfer loss caused by gas volume expansion. When temperature varies from 70 to 90 °C, the temperature effect on performance no longer follows a

linear increase but is related to the operating voltage or current density. When the current density ranges between 0-3.5 A/cm², an inlet water temperature of T_0 = 90°C results in the minimal voltage loss. However, as the current density increases, the electrolysis performance and efficiency at this temperature fall below that of T_0 = 80°C control group. When the current density exceeds 3.8 A/cm², the performance is inferior to that of T_0 = 70 °C control group. Additionally, it is observed that with a further increase in current density, the electrolysis performance at 70 °C gradually approaches that of T_0 = 80 °C. It can be projected that when the current density exceeds 4.25 A/cm², an inlet water temperature of T_0 = 70 °C will achieve the optimal electrolysis performance. This phenomenon can be attributed to the accelerated consumption rate of water on the anode side at high current densities, coupled with elevated temperatures that further expedite water evaporation. This results in a significant decrease in the membrane's water content, ultimately increasing proton transport resistance. Therefore, temperature regulation is crucial during operation at high current densities.

Fig. 4(b) illustrates that while increasing the inlet flow rate slightly enhances PEMWE performance, the improvement diminishes as the flow rate continues to rise. When the inlet water rate was increased from 0.1 to 0.9 mL/s, the average liquid water saturation in the ACL increased by 4.87%. This is because a higher inlet water rate improves the gas removal rate, resulting in better gas-liquid distribution. The effect of water flow rate on electrolysis performance becomes more significant at current densities above 2.5 A/cm², as the increased water consumption necessitates a higher flow rate to sustain the electrochemical reaction and maintain the wettability of the proton exchange membrane. However, further increasing the flow rate has a diminished effect on performance because the water, acting as a coolant, carries away more heat, thereby reducing the overall temperature of the cell.

4.2.2 Electrochemical parameters

The analysis of the electrochemical parameters is shown in Fig. 5. The effect of the anode and cathode exchange current densities on the polarization curve and PEMWE efficiency is moderate, as shown in Fig. 5(a). Quantitatively, the efficiency varies around 2.92% ($\Delta V \approx$ 0.18 V) at current density of i = 3 A/cm² when the exchange current density is varies an order of magnitude ($i_0 a_{v,a/c}$ = 5x10^{-3}-4x10^{-2}/5x10^{1}-4x10^{2}A/cm^3). The exchange current density characterizes the performance of the cathode catalyst and mainly affects the magnitude of the overpotential during the reaction as shown in Fig. 5(c). It should be noted that the margin of optimization in the anode is significantly large. A substantial increase in exchange current density of cathode (4x10^{2}-1x10^{3} A/cm^3), while maintaining a constant anode exchange current density, resulted in only a marginal enhancement in electrolysis performance.

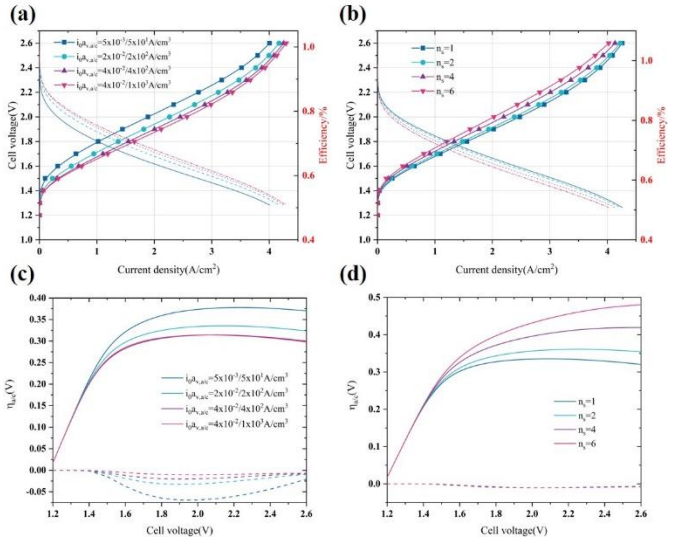

Fig. 5. Effect of different electrochemical parameters on polarization curve and efficiency, (a) $i_0 a_{v,a/c}$ = 5x10^{-3}/5x10^{1}, 2x10^{-2}/2x10^{2}, 4x10^{-2}/4x10^{2}, 4x10^{-2}/1x10^{3} A/cm^3, (b) OER coverage exponent, n_s = 1, 2, 4, 6. (c) and (d) OER/HER overpotential corresponding to (a) and (b), respectively

The n_s (1, 2, 4, 6), acting as a similar role in the Bulter-Volmer equation as the pre-factor is the exponent of the coverage factor of the OER due to gas blockage at active catalytic sites. From Fig. 5(b), under the smaller coverage factor the higher the electrolysis performance can be obtained because the catalyst has better activity and durability. The influence of the coverage factor on electrolysis performance is primarily mediated through its effect on the activation overpotential, with its impact on the cathode being negligible (n_s = 0 in the CCL), as shown in the Fig. 5(d). Effective dispersion of catalyst particles and improved liquid-gas management can reduce the coverage factor, thereby lowering the anode activation overpotential to within 0.3 V.

5. CONCLUSIONS

A steady-state, multi-phase, non-isothermal 3D model of a proton exchange membrane water electrolysis (PEMWE), implemented in commercial COMSOL Multiphysics, has been presented. The model incorporates a complete description of the conservation equations of mass, momentum, gas species, charge, dissolved water, hydrogen permeation and energy

across the membrane assembly (MEA). The model has been successfully compared in terms of polarization curves and volage loss with experimental data under different operating conditions.

Using 3-D diagrams, the study highlights the effects of water evaporation, chemical reactions, and gas diffusion on component distribution in the anode and cathode regions. It finds that increasing voltage levels lead to higher concentrations of oxygen and hydrogen, while vapor concentration decreases slightly due to accelerated condensation. The PEMWE performance enhances with increasing inlet water temperature from 50 to 70 °C due to minimized activation and Ohmic losses. Optimal performance is observed at 90 °C for current densities up to 3.5 A/cm², but declines at higher densities, where 70 °C may provide superior results due to better water management and reduced proton transport resistance. An order variation of magnitude in exchange current density leads to efficiency changes of around 2.92% at a current density of 3 A/cm², with the anode overpotential offering greater optimization potential compared to the cathode. Therefore, careful optimization of operating conditions and electrochemical parameters are essential to maximize PEMWE performance.

ACKNOWLEDGEMENT

This work was supported by National Natural Science Foundation of China (No. 52376045), and National Key Research and Development Program of China (No. 2021YFB4000100).

REFERENCE

[1] Lee JK, Anderson G, Tricker AW, Babbe F, Madan A, Cullen DA, et al. Ionomer-free and recyclable porous-transport electrode for high-performing proton-exchange-membrane water electrolysis. Nature Communications 2023;14:4592.

[2] Su C, Chen Z, Wu Z, Zhang J, Li K, Hao J, et al. Experimental and numerical study of thermal coupling on catalyst-coated membrane for proton exchange membrane water electrolyzer. Applied Energy 2024;357:122442.

[3] Falcão DS, Pinto AMFR. A review on PEM electrolyzer modelling: Guidelines for beginners. Journal of Cleaner Production 2020;261.

[4] Upadhyay M, Kim A, Paramanantham SSS, Kim H, Lim D, Lee S, et al. Three-dimensional CFD simulation of proton exchange membrane water electrolyser: Performance assessment under different condition. Applied Energy 2022;306:118016.

[5] Guan Z, Li J, Li S, Wang K, Lei L, Wang Y, et al. Multivalence-State Tungsten Species Facilitated Iridium Loading for Robust Acidic Water Oxidation. Small Methods 2024;2301419:1–11.

[6] Abdol Rahim AH, Tijani AS, Kamarudin SK, Hanapi S. An overview of polymer electrolyte membrane electrolyzer for hydrogen production: Modeling and mass transport. Journal of Power Sources 2016;309:56–65.

[7] Toghyani S, Afshari E, Baniasadi E. Metal foams as flow distributors in comparison with serpentine and parallel flow fields in proton exchange membrane electrolyzer cells. Electrochimica Acta 2018;290:506–19.

[8] Olesen AC, Frensch SH, Kær SK. Towards uniformly distributed heat, mass and charge: A flow field design study for high pressure and high current density operation of PEM electrolysis cells. Electrochimica Acta 2019;293:476–95.

[9] Chen Q, Wang Y, Yang F, Xu H. Two-dimensional multi-physics modeling of porous transport layer in polymer electrolyte membrane electrolyzer for water splitting. International Journal of Hydrogen Energy 2020;45:32984–94.

[10] Lin N, Zausch J. 1D multiphysics modelling of PEM water electrolysis anodes with porous transport layers and the membrane. Chemical Engineering Science 2022;253:117600.

[11] García-Salaberri PA. 1D two-phase, non-isothermal modeling of a proton exchange membrane water electrolyzer: An optimization perspective. Journal of Power Sources 2022;521:230915.

[12] Majasan JO, Cho JIS, Dedigama I, Tsaoulidis D, Shearing P, Brett DJL. Two-phase flow behaviour and performance of polymer electrolyte membrane electrolysers: Electrochemical and optical characterisation. International Journal of Hydrogen Energy 2018;43:15659–72.